EPJ Photovoltaics **4**, 40301 (2013)
www.epj-pv.org
DOI: 10.1051/epjpv/2012012

Performance potential of low-defect density silicon thin-film solar cells obtained by electron beam evaporation and laser crystallisation

J. Dore[1,2], S. Varlamov[2,a], R. Evans[1], B. Eggleston[1,2], D. Ong[1], O. Kunz[1], J. Huang[2], U. Schubert[1], K.H. Kim[1,2], R. Egan[1], and M. Green[2]

[1] Suntech R&D Australia, Pty., Ltd. 82-86 Bay St., Botany, NSW 2019, Australia
[2] University of NSW Sydney, NSW 2052, Australia

Received: 30 July 2012 / Received in final form: 26 November 2012
Published online: 11 January 2013

Abstract A few microns thick silicon films on glass coated with a dielectric intermediate layer can be crystallised by a single pass of a line-focused diode laser beam. Under favorable process conditions relatively large linear grains with low defect density are formed. Most grain boundaries are defect-free low-energy twin-boundaries. Boron-doped laser crystallised films are processed into solar cells by diffusing an emitter from a phosphorous spin-on-dopant source, measuring up to 539 mV open-circuit voltage prior to metallisation. After applying a point-contact metallisation the best cell achieves 7.8% energy conversion efficiency, open-circuit voltage of 526 mV and short-circuit current of 26 mA/cm^2. The efficiency is significantly limited by a low fill-factor of 56% due to the simplified metallisation approach. The internal quantum efficiency of laser crystallised cells is consistent with low front surface recombination. By improving cell metallisation and enhancing light-trapping the efficiencies of above 13% can be achieved.

1 Introduction

Crystalline silicon (c-Si) wafer-based solar cells dominate the photovoltaic (PV) market due to the mature and constantly improving technology and a decreasing manufacturing cost. One of the major contributors into cost reduction is the use of thinner cells to lower the consumption of the material. A number of approaches exist to produce thin c-Si wafers and layers [1]. c-Si films on supporting substrates such as glass is one of such approaches and a few technologies have been developed to produce solar cells from such films [2–6]. The highest module efficiency of c-Si thin-film solar cells on glass is 10.5% [4]. Further improvement in the cell performance is limited by the high density of intragrain defects and related poor electronic quality of the material [7, 8] typically obtained by solid-phase crystallisation (SPC) or epitaxy (SPE) at relatively low temperatures compatible with the glass substrate. A new approach has recently emerged that exploits zone-melt-like liquid-phase crystallisation (LPC) of precursor silicon films by an electron beam to produce large-grained and low-defect density c-Si films on glass with the superior electronic quality compared to SPC silicon [9, 10]. The open circuit voltage (V_{OC}) of 545 mV and the efficiency of 4.7% were demonstrated for a cell with a LPC absorber and an a-Si:H heterojunction emitter. This paper presents initial results for a similar approach but where a diode laser is used for the LPC to obtain high crystallographic and electronic quality Si films. These films are processed into 7.8% efficient cells with a diffused homojunction emitter.

2 Experiment

Planar Schott Borofloat33 glass was used as a substrate for film deposition. It was coated with an intermediate dielectric layer, such as SiC_x, SiO_x, SiN_x or their combination. These layers, intrinsic or boron-doped, were prepared by RF magnetron sputtering or co-sputtering using dielectric and pure boron targets. Then, 10 μm thick Si films, undoped or boron doped at 1E16 cm^{-3}, were deposited by electron-beam evaporation at 650 °C on boron-doped or undoped intermediate layer respectively. The Si films were crystallised by a single pass of a line-focus beam from an 808 nm CW diode laser, LIMO450-L12 × 0.3-DL808-EX937. The laser beam has a Gaussian profile in

[a] e-mail: s.varlamov@unsw.edu.au

the short (scan) direction (FWHM 0.170 mm) and a top-hat profile in the long direction (FWHM 12 mm). The laser conditions were 15–25 kW/cm^2 and 10–15 ms exposure time at sample stage pre-heat temperature in the range of 550–700 °C. Solar cells of 1.7 × 0.6 cm^2 size were fabricated in the middle of the crystallised strips. The cell emitter was formed by phosphorous diffusion at about 900 °C from a spin-on source. The hydrogen plasma passivation and metallisation processes applied to the cells are similar to those used for SPC Si thin-film solar cells [4–6]. Metallisation relies on forming point contacts on the rear side of the device by inkjet printing holes in a resin layer and then etching down to the emitter and absorber layers in sequence. Sputtered Al is then used to form contacts to the n- and p-type openings. This metallisation is very similar to the one described in [11] but simplified by reducing the contact density and no heavy Si doping under the p-type contacts to the absorber to accommodate and facilitate quicker cell development. Current research-level planar cells rely on a pigmented rear diffuse reflector for modest light-trapping.

The Si film crystal quality was characterised by SEM and TEM imaging. The dopant concentration in the films was estimated from SIMS measurements. The electronic film quality and the cell performance was characterised by Hall measurements, Suns-V_{oc}, Light I-V and spectral response techniques.

3 Results and discussion

A few micron thick e-beam evaporated Si films can be crystallised in a quick, zone-melt like process by scanning with a high power line-focus diode laser beam. Continuous lateral crystal growth can be achieved whereby the growth front is seeded by the preceding crystallised region, forming long parallel grains in the direction of scanning (Fig. 1). Factors having significant effects on the crystallisation process include an intermediate layer between glass and Si, laser beam parameters and the substrate temperature during crystallisation.

3.1 Intermediate layer

The intermediate layer has to be stable at the Si melting point of 1414 °C and it serves a few important functions: enables molten Si to wet substrate sufficiently to avoid balling up; blocks impurity diffusion from glass; acts as a dopant source; provides an antireflection (AR) effect; and passivates the front device surface (the Si-glass interface). Transparent dielectric films, SiO_x, SiC_x, and SiN_x, and their different combinations were tested as the intermediate layers, along with their interactions with laser beam parameters. Properties of different intermediate layers and their effects on cell performance are described in detail elsewhere [11,12]. No single layer alone can perform all required functions. SiC_x (refractive index $(n) = 2.9$) is the best wetting layer providing the widest laser process window but it allows impurity diffusion from glass, absorbs too much of the short wavelength light <500 nm, and it does not passivate the Si-glass interface well (Sect. 3.4). SiO_x is the best impurity diffusion barrier and the surface passivating layer resulting in the highest V_{OC} but because its refractive index is very similar to that of the superstrate glass ($n = 1.51$) it does not offer any additional AR effect to that already provided by the glass alone and it has the smallest laser process window. SiN_x ($n = 2.11$) offers the best AR effect and a reasonably wide laser parameter widow but it leads to pinholing and the poorest cell performance. Only a combination of different dielectrics is proved to deliver a satisfactory process and cell performance. Results presented in this report are obtained using a three layer stack of $SiO_x/SiC_x/SiO_x$ (O/C/O, 80 nm, 14 nm, 15 nm respectively). The oxide layers in the stack are boron-doped at a level of $4 \sim 5E19$ cm^{-3} (estimated from SIMS measurements) such that after boron diffusion that occurs during laser melting the sheet resistance of crystallised Si films is about 2 000 Ω/sq and the boron concentration of about 1E16 cm^{-3}.

3.2 Laser process

The range of laser parameters that allows a successful crystallization process is limited by the resulting Si crystal structure at the lower energy-dose end, which has to avoid amorphous and/or microcrystalline material, and by dewetting of a Si film from the substrate at the high dose end. Without any intermediate wetting layer, and without substrate heating dewetting and/or delamination occurs at energy doses comparable with the crystallisation limit and no process is feasible.

With the intermediate layer, a large-grained crystalline silicon material without dewetting or delamination is obtained at substrate temperatures exceeding the glass softening point of about 550 °C and the minimum laser energy dose of 220 J/cm^2. The experimentally determined process window for the dose is about 250, 220 and 190 J/cm^2 wide for the SiC_x, SiN_x and SiO_x, intermediate layer respectively. The cells on the O/C/O intermediate layer coated glass presented in this report typically require the energy dose of 240–260 J/cm^2.

3.3 Structural quality

The optimised laser crystallisation process results in lateral growth of linear silicon grains which extend through the whole film thickness of 10 μm and they are a few millimetres long and 50–500 μm wide (Fig. 1). According to electron backscatter diffraction (EBSD) most of the linear grains have [101] orientation in direction normal to the film plane [13]. TEM cross-sectional images and their corresponding diffraction patterns (Figs. 2, 3) confirm complete crystallisation with [110] grain orientation in direction parallel to the film. It is consistent with the EBSD images from [13] as EBSD and TEM are measured at approximately 90° relative to each other. The silicon grains contain regions with the varying defect density which was evaluated by counting dislocation lines

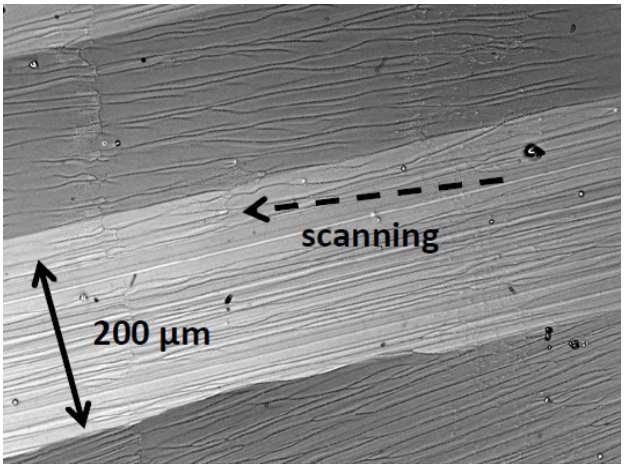

Fig. 1. Backscatter SEM image of lateral grains in diode laser crystallised Si film. ∼200 μm-wide linear grains are shown in the same shade of grey; wavy lines within each grain are surface texture developed during crystallisation while straight parallel lines are twin boundaries.

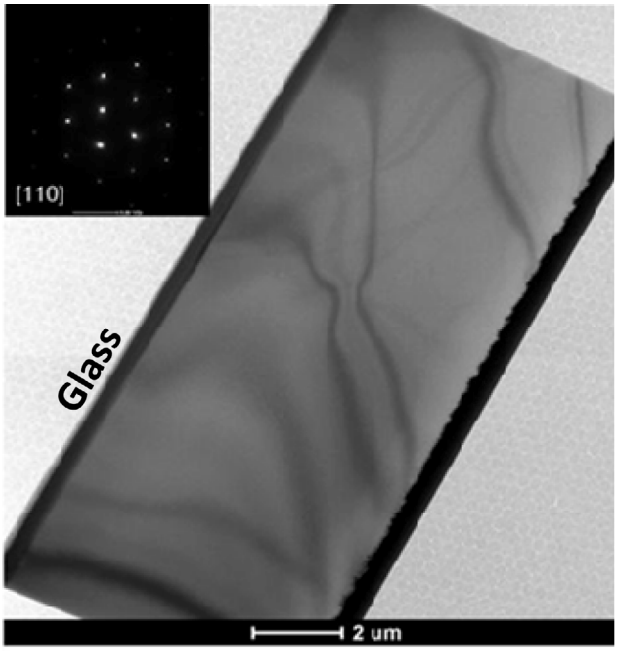

Fig. 2. TEM image and diffraction pattern of defect-free grain with [110] orientation in diode laser crystallised Si film.

in Weak-Beam-Dark-Field (WBDF) images. Most laterally grown grains are nearly defect-free on the TEM scale which translates into the defect density of 1E5 cm^{-2} or lower (Fig. 2) while the most defect-rich grains can contain dislocations with the density up to 1E9 cm^{-2} (Fig. 3). The most commonly observed boundaries between linear grains are defect-free low-energy $\Sigma 3$ twin-boundaries which are electrically inactive, i.e. they do not significantly contribute into carrier recombination [10, 14].

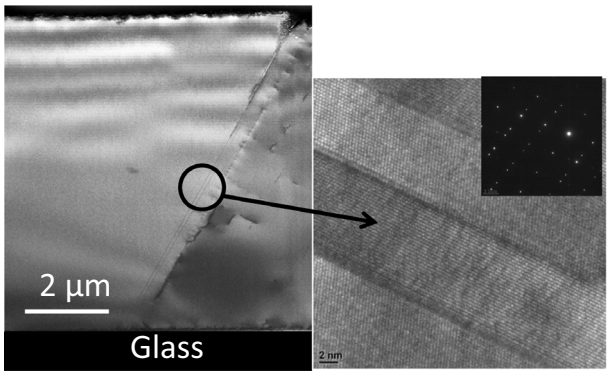

Fig. 3. (Left) TEM image of diode laser crystallised Si grains with twin boundary (circle) and dislocations; (right) high resolution TEM image of defect-free twin boundary.

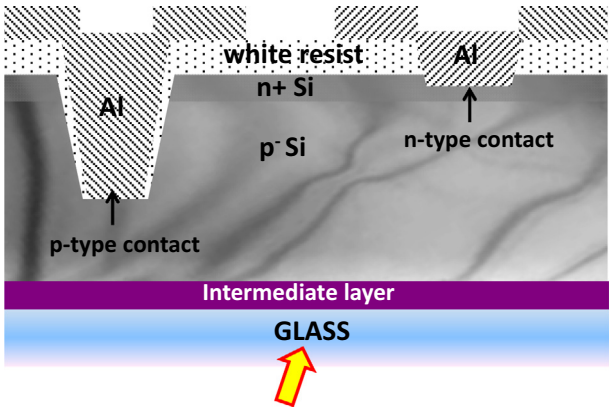

Fig. 4. The structure of a metallised solar cell. The light enters the cell through the front, glass side.

3.4 Electronic properties and cell performance

The carrier mobility, concentration and bulk resistivity of laser crystallised boron-doped Si films used for cell fabrication were calculated from Hall effect measurements using the Van der Pauw cross pattern. Depending on a particular location the mobility typically varies between 300 and 470 cm^2/V s, the carrier concentration ∼10E16 cm^{-3}, and resistivity 1–3 Ω cm. These values are similar to those measured for a reference c-Si wafer: 414 cm^2/V s, 1.6E16 cm^{-3}, 0.94 Ω cm respectively, indicating a high electronic quality of the laser crystallised silicon film, which is a lot better than the quality of a reference SPC Si film with a similar boron concentration and a mobility of 50–120 cm^2/V s, which is in agreement with the mobilities of 40–90 cm^2/V s reported elsewhere [15].

The structure of a metallised solar cell is shown in Figure 4.

The cell voltages depend on the intermediate dielectric layers, which is discussed elsewhere [11, 12]. The cells on SiO_x achieve V_{OC} in a range of 520–540 mV, while the cells on SiN_x have the poorest V_{OC}, below 500 mV. These effects are not well understood but it can be speculated that the oxide provides the best silicon-glass interface passivation which is consistent with high blue response for cells on SiO_x (Fig. 5, right). For cells on SiN_x SIMS data indicate

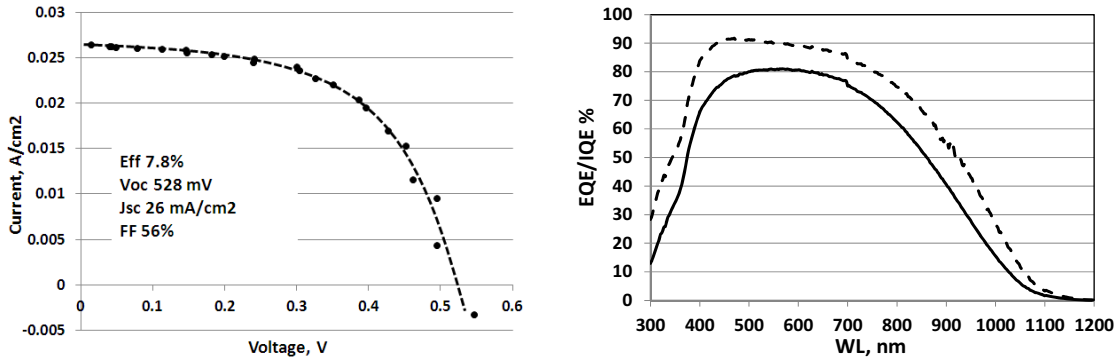

Fig. 5. (Left) Light *I-V* curve and (right) *EQE* (solid) and *IQE* (broken) of 7.8% efficient laser crystallised Si thin-film cell.

presence of nitrogen contamination which can be negatively affecting the voltages. The best performing metallised 7.8%-efficient cell on the O/C/O triple layer stack has V_{OC} of 526 mV, similar to V_{OC} of the cells on the oxide only but an improvement in cell antireflection properties due to presence of a very thin SiC_x layer on the front leads to a significant current gain, 26 mA/cm^2 versus 24 mA/cm^2 for the cell on SiO_x [11].

The light *I-V* curve of the best, 7.8% efficient cell is shown in Figure 5 (left).

The series and shunt resistances (R_s and R_{sh}) of 4.5 and 317 $\Omega\,\mathrm{cm}^2$ respectively, were estimated by measuring the inverse slope of the *I-V* curve at the voltage and current axes. High R_s is due to poor metal contacts that are made to lightly-doped (∼1E16 cm^{-3}) silicon. It is also possible that a Schottky diode is formed at such contacts, which has a negative contribution to the cell voltage [16]. A source of relatively low R_{sh} is not yet identified. Both high R_s and low R_{sh} result in the low *FF* of 56%. It can be shown [17] that R_s of 4.5 $\Omega\,\mathrm{cm}^2$ results in the *FF* reduction of about 13%, from nominal 70%, typical for poly-Si thin-film cells with a similar metallisation scheme and R_s of 1.3 $\Omega\,\mathrm{cm}^2$ [4,6], to 57%, in a good agreement with the measured *FF* value. It is also estimated that R_{sh} of 317 $\Omega\,\mathrm{cm}^2$ can be responsible for only about 3% reduction in the *FF*. Both these issues can be addressed by improving cell metallisation, for example, by selectively doping the contacts to the absorber. With the *FF* of at least 70%, which is typical for optimised contact schemes of this type [18], the cell efficiency would approach 10%.

The *EQE,* and *IQE* curves of the best cell are shown in Figure 5 (right). The *IQE* is adjusted to take into account parasitic absorption in the SiC_x layer, which was measured prior to silicon deposition, as presented in [11]. The *IQE* peaks at around 90% and it stays around this value for most of the visible wavelength range. For a rear-junction cell it suggests the low front surface recombination velocity and the minority carrier diffusion length greater than the cell thickness of 10 μm.

3.5 Performance potential

In order to estimate the performance potential of the laser crystallised silicon material the cell *IQE* was fitted by using PC1D modelling. This allows indicative values of bulk lifetime (τ) and front surface recombination velocity (S_F) to be extracted. The rear-surface recombination velocity was found to have no impact on the *IQE* in this model, which is likely due to the low minority carrier concentration at the heavily doped n+ rear surface.

The best 7.8% efficient cell is difficult to model because of complexity of its optical properties in the short-wavelength region due to presence of the triple O/C/O intermediate layer stack on the front. Instead, a similar cell but on the single SiO_x layer was used. It is justified because both cells have similar V_{OC} and similarly high *IQE* in the visible region (Figs. 5 and 6). The oxide film and the glass were treated as one 3.3 mm thick layer with the refractive index of 1.5.

Possible ranges for τ and S_F can be estimated by looking at two extreme cases. The case when recombination is dominated by the front surface can be modelled by setting τ very high (e.g. 100 μs). In this case, a good *IQE* fit with maximum of 93% is achieved when $S_F = 1900$ cm/s or less (blue dotted line in Fig. 6). Similarly, the case dominated by bulk recombination is modelled by setting S_F very low (e.g. to 100 cm/s). In this case, a good *IQE* fit is obtained when $\tau = 260$ ns or more (purple dotted line in Fig. 6). Thus, we can conclude from using this model that τ is at least 260 ns, and that S_F is at most 1900 cm/s. At present, there is no indication as to which case, bulk or surface recombination, limits the cell performance. The parameters used to obtain the best fits are listed in Table 1.

Even at the minimum value of 260 ns, the lifetime would be sufficient for significantly higher efficiencies, should all other device properties be optimised. This is instructive because it shows that the achieved cell performance is not limited by the laser crystallised material quality and thus identifies device optimisation as the immediate development priority leading to better cell performance, rather than the silicon material itself. For example, an ideal cell with R_s of 1–1.5 $\Omega\,\mathrm{cm}^2$ (e.g. with selectively doped absorber contacts), no shunts, optimum antireflection coating and internal reflectance of over 90% (e.g. via light-trapping by surface texture as described in [19]) would be potentially capable of an efficiency of over 13%.

Table 1. PC1D model parameters.

Thickness [μm]	10
p-type background doping [cm^{-3}]	7E15
Peak n-type emitter doping [cm^{-3}]	1.5E19
Bulk lifetime [μs] (bulk-limited; $S_F = 100$ cm/s)	0.26
Rear-surface recombination velocity [cm/s]	1E4
Front-surface recombination velocity [cm/s] (surface-limited, $\tau = 100$ μs)	1900
Front internal reflectance [%]	51
Rear internal reflectance [%]	58

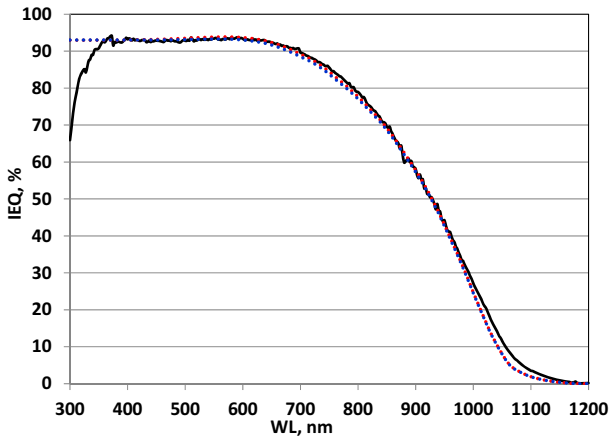

Fig. 6. Experimental (black-solid line) *IQE* curve and front-surface (blue-dotted line) and bulk recombination (red-dotted line) limited model fits of the cell on the oxide layer.

4 Conclusions

It is demonstrated than line-focused diode laser crystallisation of a few micron thick silicon films on glass can produce a high crystal and electronic quality material. Such a material consists of a few millimetre long and 50–500 micron wide grains with low defect density. The majority of grains boundaries are defect free low-energy $\Sigma 3$ twin boundaries. Laser process parameters, crystal and electronic film and cell properties are influenced by an intermediate dielectric layer between glass and silicon. Solar cells with a diffused emitter that are fabricated on the SiO_x layer achieve the highest V_{OC} up to 539 mV. The cells on the $SiO_x/SiC_x/SiO_x$ triple stack layer achieve the best efficiency up to 7.8%. The performance is not limited by the quality of the laser crystallised Si material but by simplified device design and poor light-trapping. PC1D modelling suggests a bulk lifetime of at least 260 ns, which in an otherwise optimised device, would be compatible with efficiencies of over 13%. Future work will focus on device optimisation to determine how much of this improvement is achievable.

References

1. F.J. Henley, in *Proceedings of the IEEE Photovoltaic Specialist Conference, Honolulu, USA, 2010*, p. 1184
2. H.M. Branz, C.W. Teplin, M.J. Romero, I.T. Martin, Q. Wang, K. Alberti, D.L. Young, P. Stradin, Thin Solid Films **519**, 4545 (2011)
3. I. Gordon, L. Carnel, D. Van Gestel, G. Beaucarne, J. Poortmans, Prog. Photovolt.: Res. Appl. **15**, 574 (2007)
4. M. Keevers, T. Young, U. Schubert, M. Green, in *Proceedings of the 22 European Photovoltaic Solar Energy Conference, Milan, Italy, 2007*
5. O. Kunz, Z. Ouyang, S. Varlamov, A. Aberle, Prog. Photovolt.: Res. Appl. **17**, 567 (2009)
6. R. Egan et al., in *Proceedings of the 24 European Photovoltaic Solar Energy Conference, Hamburg, Germany, 2009*
7. J. Wong, J. Huang, B. Eggleston, M.A. Green, O. Kunz, R. Evans, M. Keevers, R.J. Egan, J. Appl. Phys. **107**, 123705 (2010)
8. J. Wong, J. Huang, S. Varlamov, M. Green, M. Keevers, Prog. Photovolt.: Res. Appl. (2011), DOI: 10.1002/pip.1154
9. D. Amkreutz, J. Muller, M. Schmidt, T. Hanel, T.F. Schulze, Prog. Photovolt.: Res. Appl. **19**, 937 (2011)
10. W. Seifert, D. Amkreutz, T. Arguirov, M. Krause, M. Schmidt, Solid State Phenomena **178-179**, 116 (2011)
11. J. Dore, R. Evans, U. Schubert, B. Eggleston, D. Ong, K. Kim, J. Huang, O. Kunz, M. Keevers, R. Egan, S. Varlamov, M. Green, Prog. Photovolt.: Res. Appl., DOI: 10.1002/pip.2282
12. J. Dore, R. Evans, B. Eggleston, S. Varlamov, M. Green, MRS Online Proceedings Library **1426** (2012), Doi:10.1557/opl.2012.866
13. B. Eggleston, S. Varlamov, J. Huang, R. Evans, J. Dore, M. Green, MRS Online Proceedings Library **1426** (2012), Doi:10.1557/opl.2012.1260
14. J. Chen, T. Sekiguchi, D. Yang, F. Yin, K. Kido, S. Tsurekawa, J. Appl. Phys. **96**, 5490 (2004)
15. T. Noguchi, Jpn J. Appl. Phys. **32**, L1584 (1993)
16. S.W. Glunz, J. Nekarda, H. Mäckel, A. Cuevas, in *Proceedings of the 22 European Photovoltaic Solar Energy Conference, Milan, Italy, 2007*, p. 849
17. M.A. Green, *Solar Cells* (University of NSW, 1992), p. 97
18. S. Partlin, N. Chang, R. Egan, T. Young, D. Kong, R. Evans, D.A. Clugston, P. Lasswell, A. Turner, J. Dore, T. Florian, in *Proceedings of the 25 European Photovoltaic Solar Energy Conference, Valencia, Spain, 2010*, p. 3568
19. Q. Wang, T. Soderstrom, K. Omaki, A. Lennon, S. Varlamov, Energy Procedia **15**, 220 (2012)

Cite this article as: J. Dore, S. Varlamov, R. Evans, B. Eggleston, D. Ong, O. Kunz, J. Huang, U. Schubert, K.H. Kim, R. Egan, M. Green, Performance potential of low-defect density silicon thin-film solar cells obtained by electron beam evaporation and laser crystallisation, EPJ Photovoltaics **4**, 40301 (2013).